Epigenetic changes in human model KMT2A leukemias highlight early events during leukemogenesis

Thomas Milan,[1] Magalie Celton,[1] Karine Lagacé,[1] Élodie Roques,[1] Safia Safa-Tahar-Henni,[1] Eva Bresson,[2,3] Anne Bergeron,[2,3] Josée Hebert,[4,5] Soheil Meshinchi,[6] Sonia Cellot,[7] Frédéric Barabé[2,3,8] and Brian T. Wilhelm[1,5]

[1]Laboratory for High Throughput Biology, Institute for Research in Immunology and Cancer, Montréal, Québec, Canada; [2]Centre de Recherche en Infectiologie du CHUL, Centre de Recherche du CHU de Québec Université Laval, Québec City, Québec, Canada; [3]CHU de Québec Université Laval Hôpital Enfant-Jésus, Québec City, Québec, Canada; [4]Division of Hematology-Oncology and Leukemia Cell Bank of Quebec, Maisonneuve-Rosemont Hospital, Montréal, Québec, Canada; [5]Department of Medicine, Université de Montréal, Montréal, Québec, Canada; [6]Clinical Research Division, Fred Hutchinson Cancer Research Center, Seattle, Washington, PA, USA; [7]Department of Pediatrics, Division of Hematology, Ste-Justine Hospital, Montréal, Québec, Canada and [8]Department of Medicine, Université Laval, Quebec City, Québec, Canada

 doi:10.3324/haematol.2020.271619

Received: September 7, 2020.

Accepted: December 21, 2020.

Pre-published: December 30, 2020.

Correspondence: *BRIAN T. WILHELM* - brian.wilhelm@umontreal.ca

a

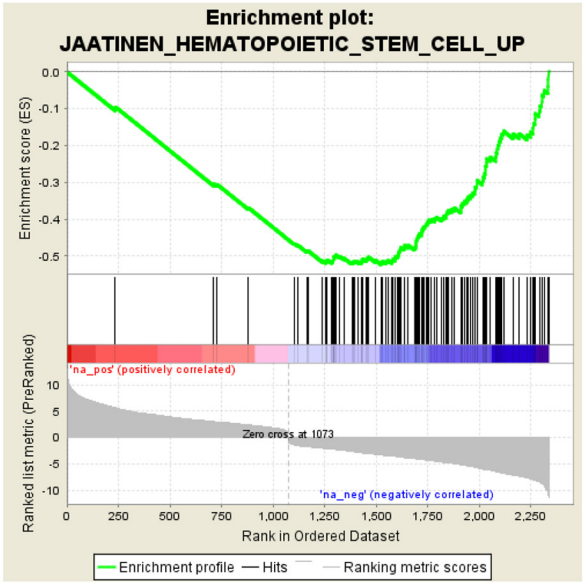

GeneSet	JAATINEN_HEMATOPOIETIC_STEM_CELL_UP
Enrichment Score (ES)	-0.5234885
Normalized Enrichment Score (NES)	-3.1416063
Nominal p-value	0.0
FDR q-value	0.0
FWER p-Value	0.0

b

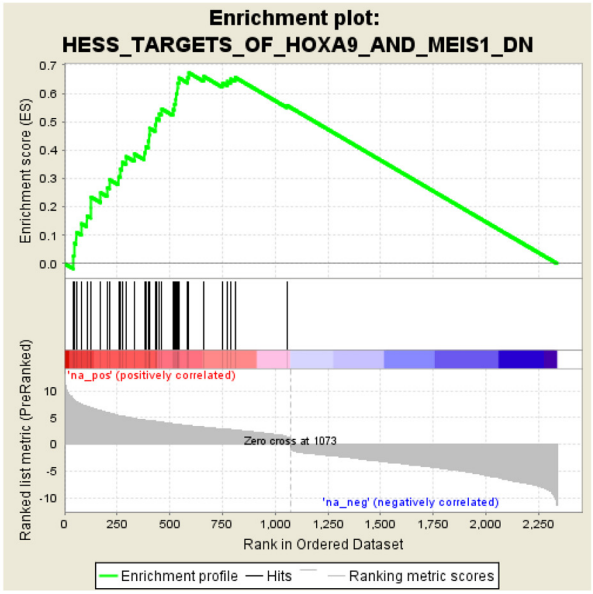

GeneSet	HESS_TARGETS_OF_HOXA9_AND_MEIS1_DN
Enrichment Score (ES)	0.67227644
Normalized Enrichment Score (NES)	3.4345574
Nominal p-value	0.0
FDR q-value	0.0
FWER p-Value	0.0

Supplemental figure 1

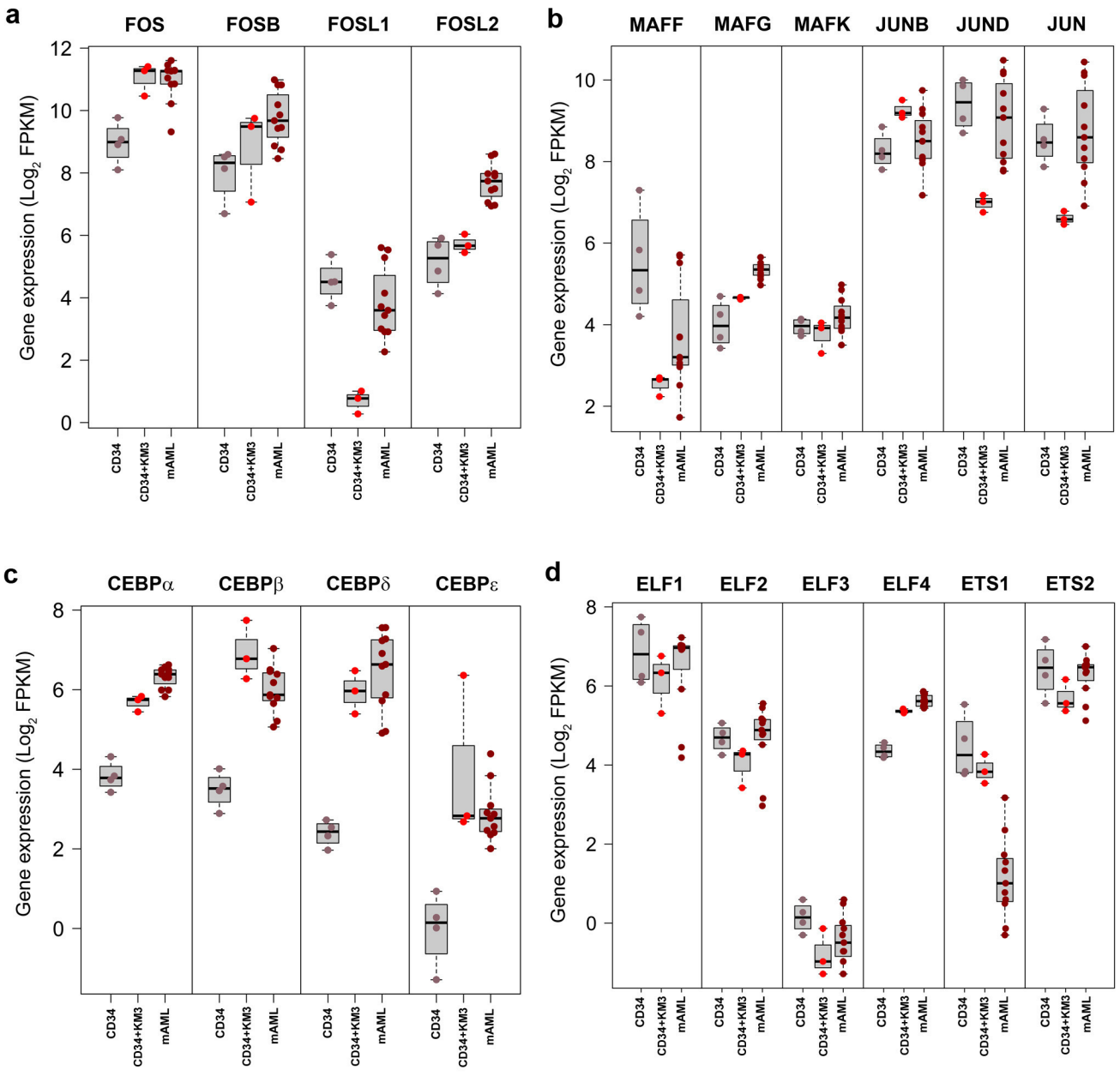

Supplemental figure 2

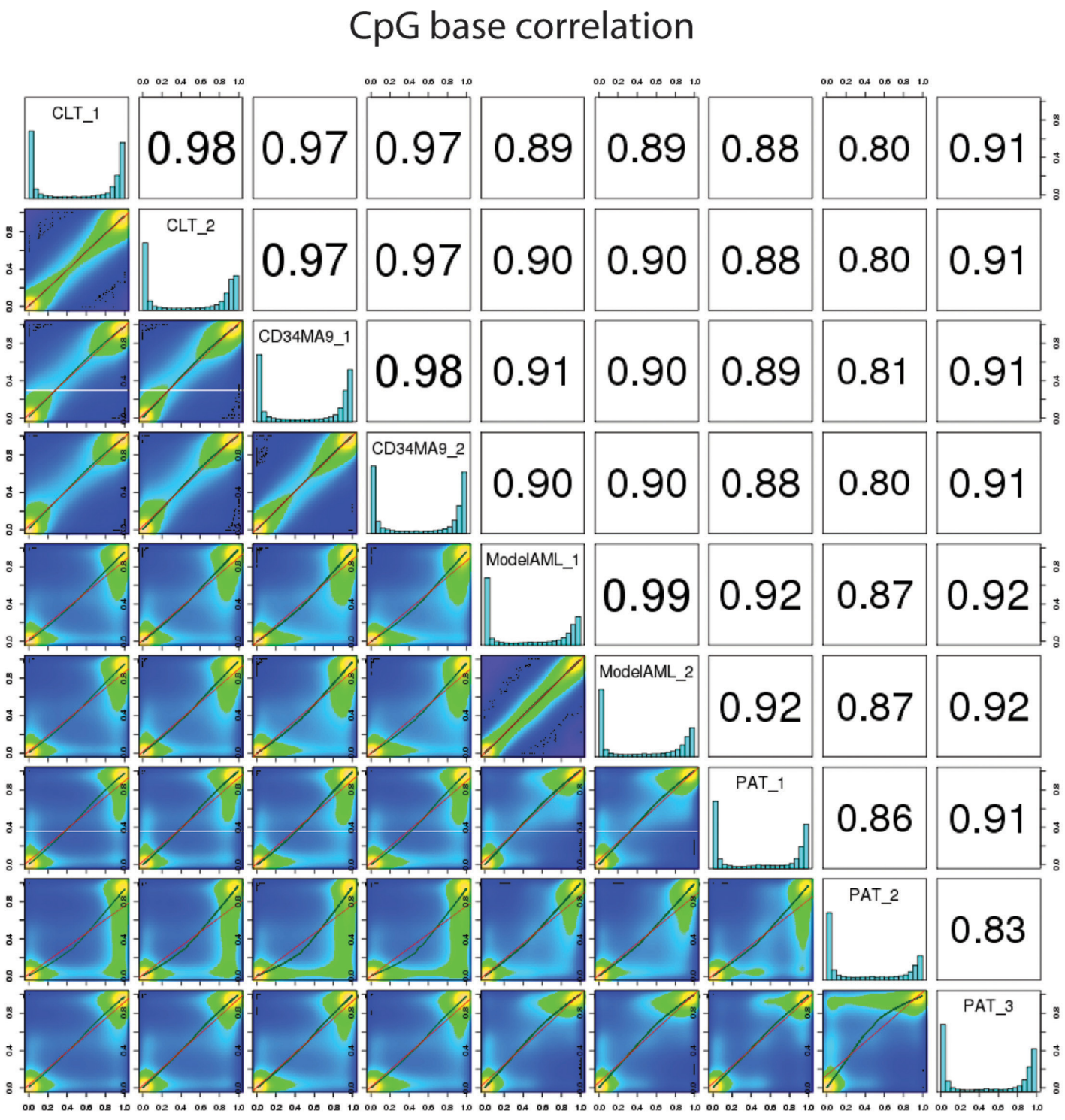

Supplemental figure 3

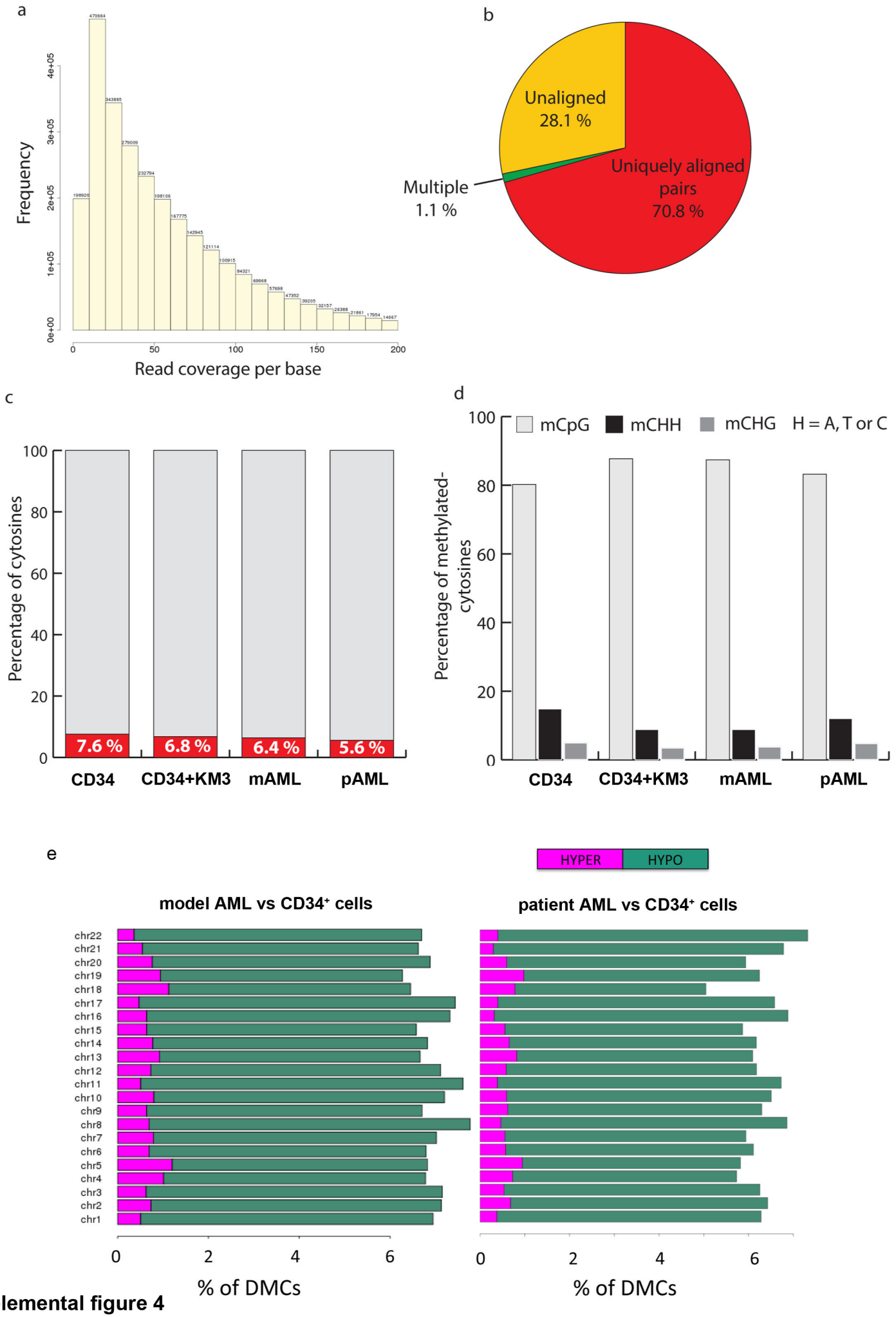

Supplemental figure 4

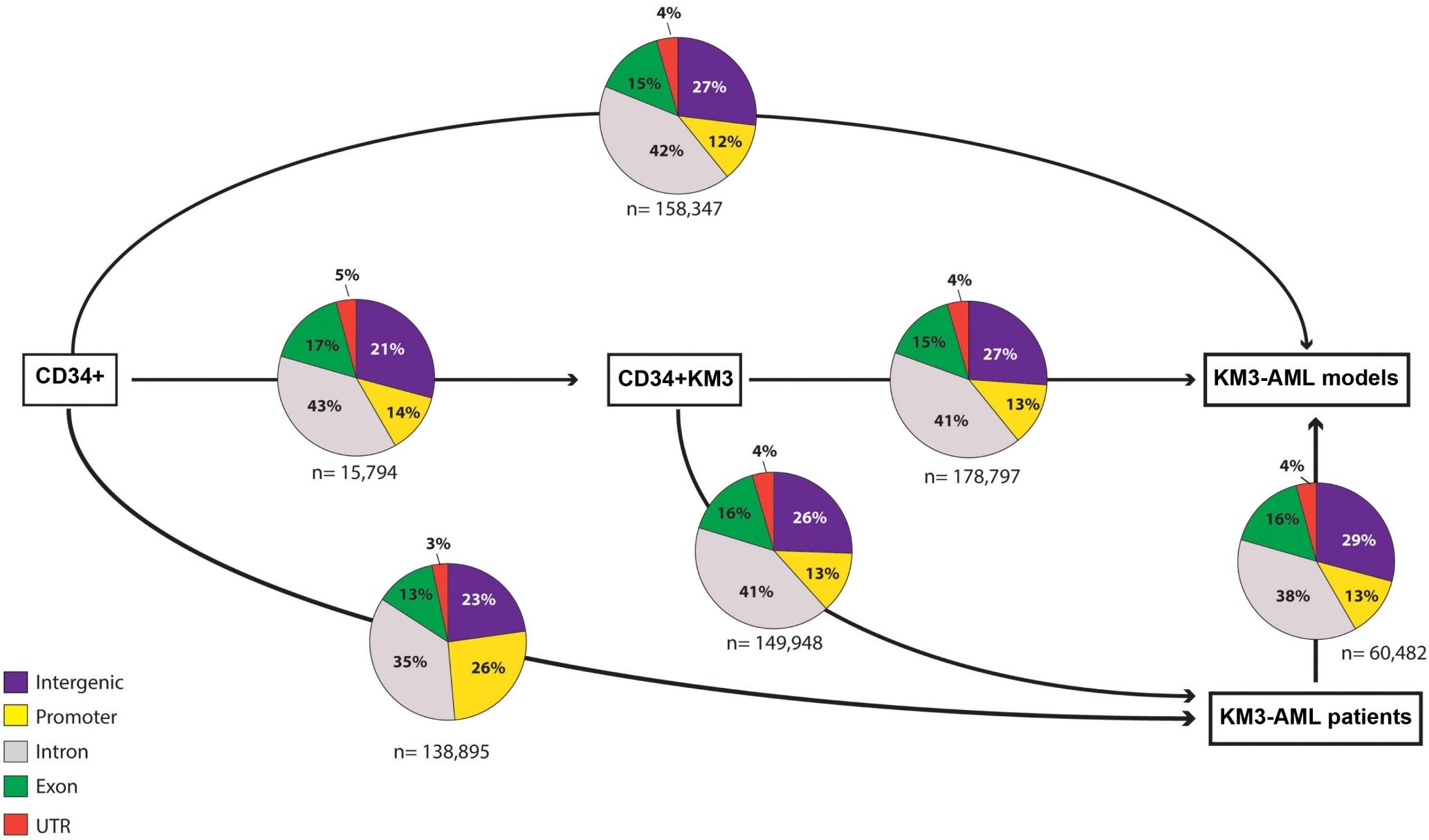

Supplemental figure 5

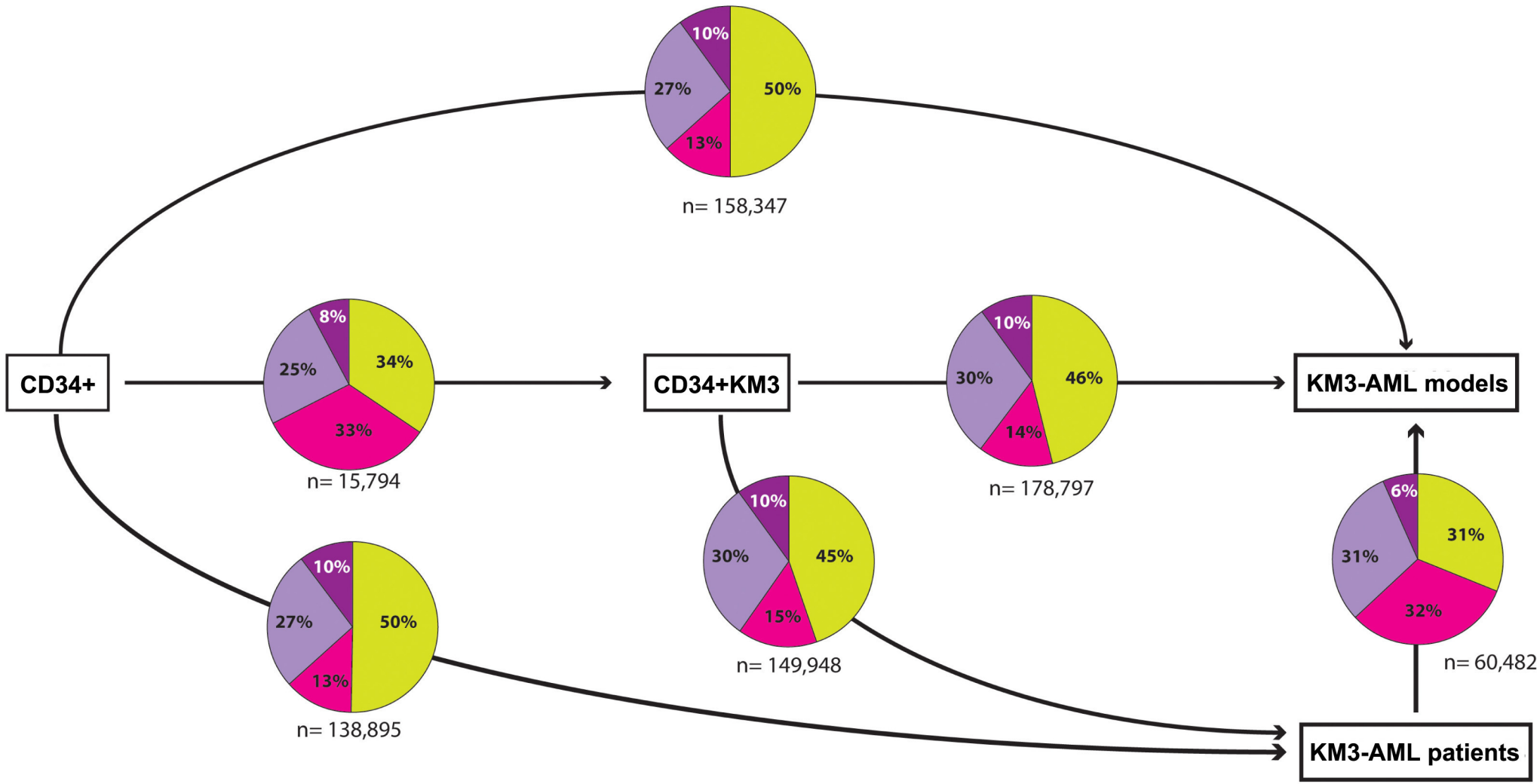

Supplemental figure 6

a

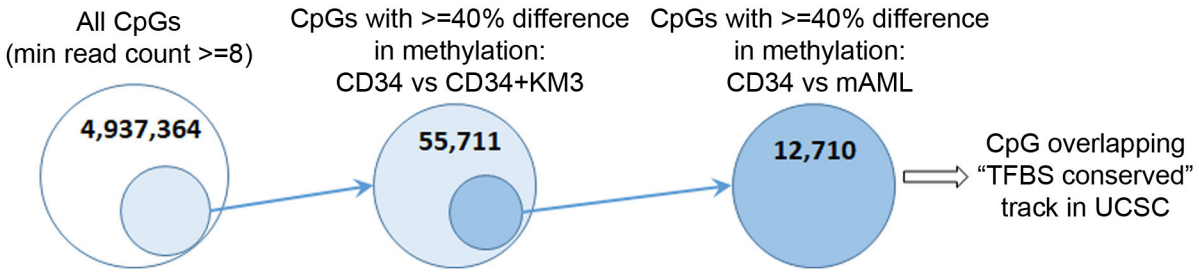

b

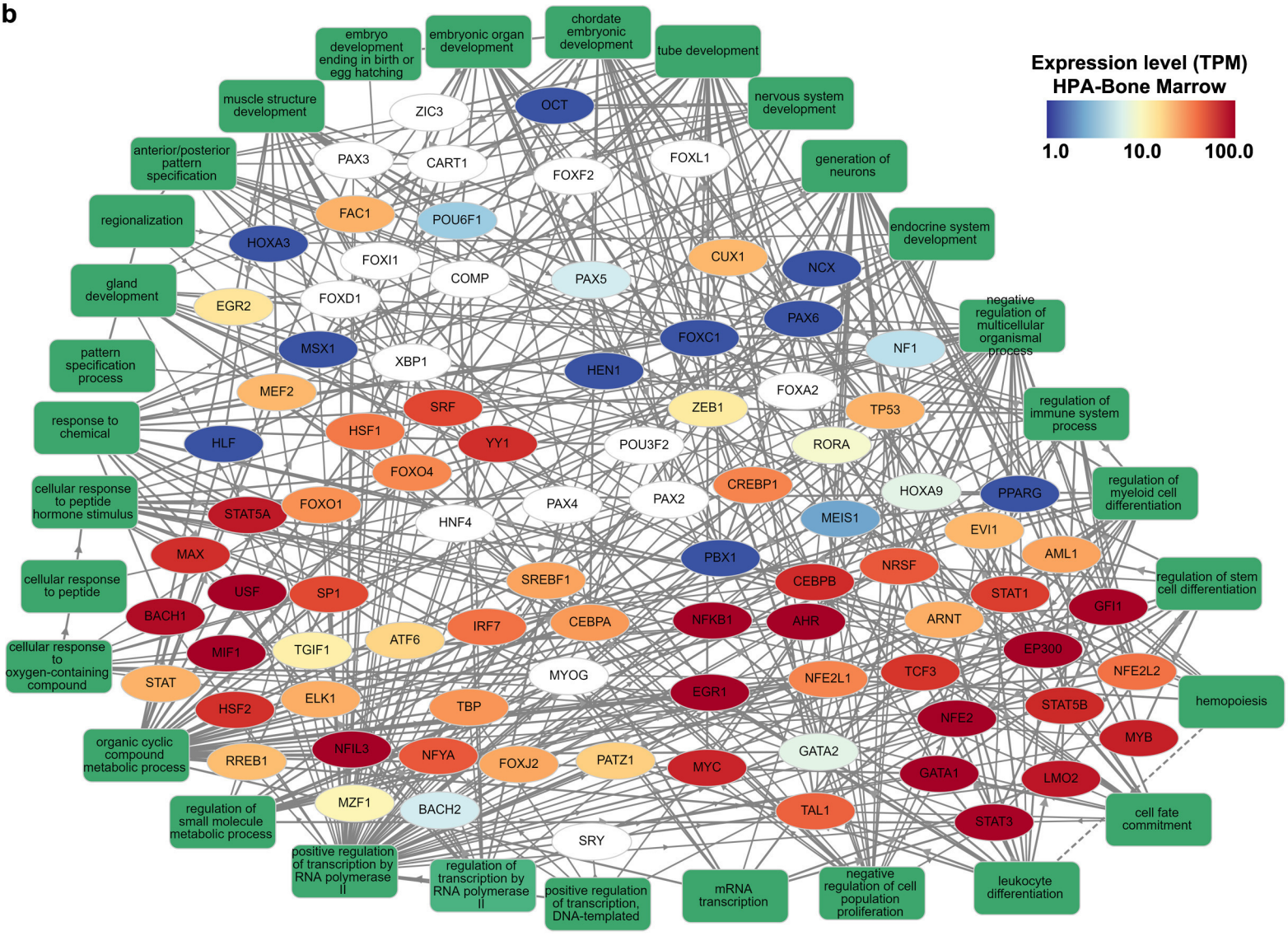

Supplemental figure 7

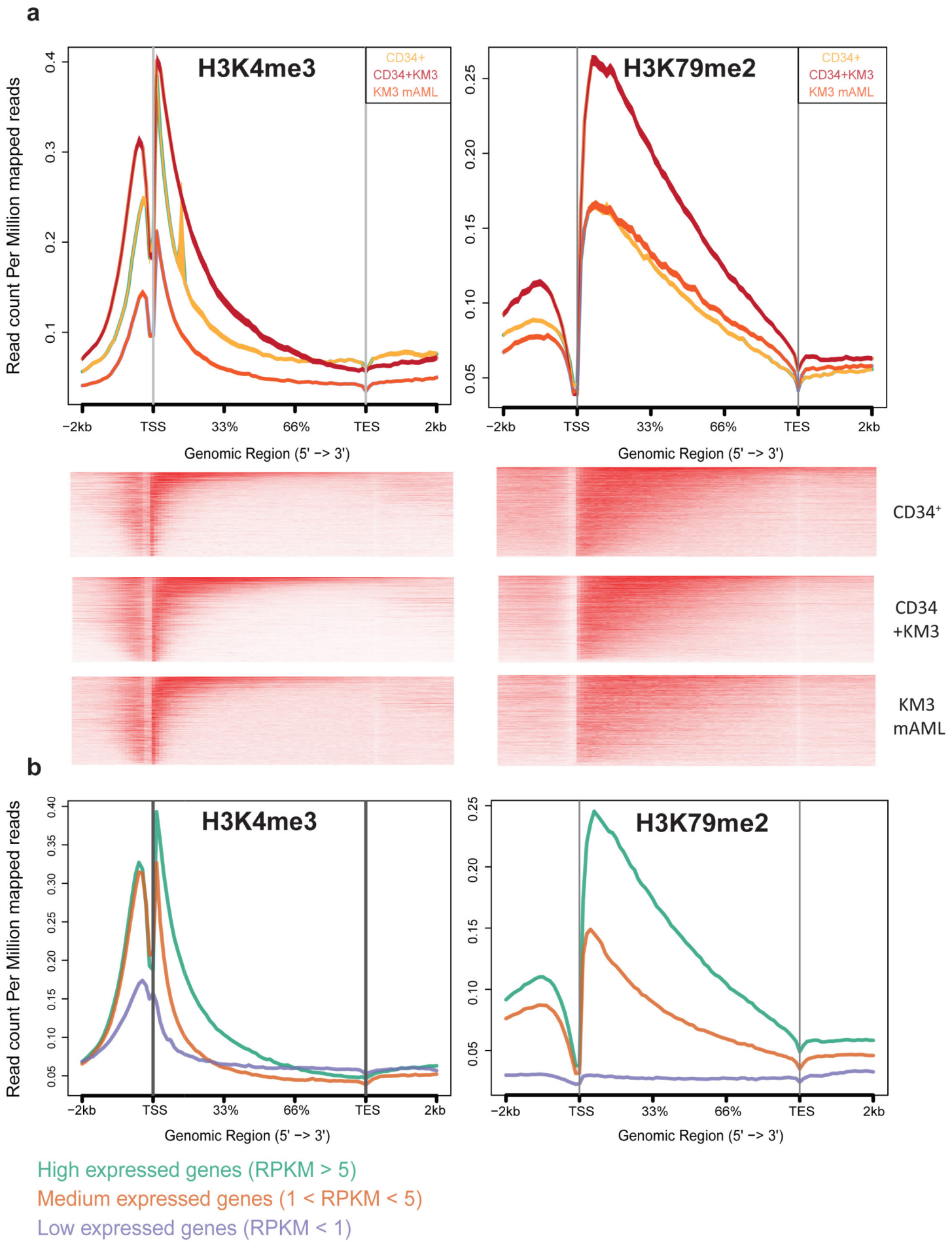

Supplemental figure 8

a

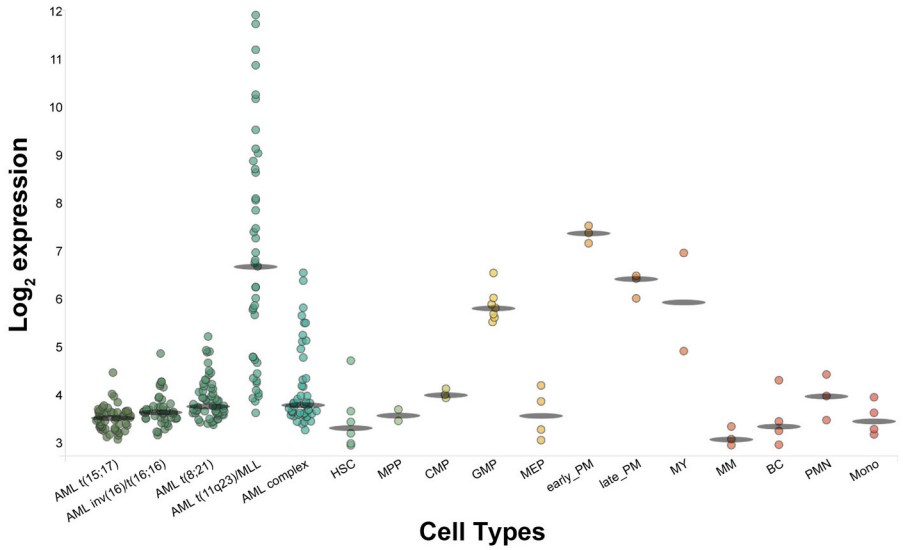

Human Normal Hematopoiesis are cells are from GSE42519
Human AML cells are from GSE13159

Abbreviation	Name	Immunophenotype
AML t(15;17)	AML with t(15;17)	Whole BM unsorted
AML inv(16)/t(16;16)	AML with inv(16)/t(16;16)	Whole BM unsorted
AML t(8;21)	AML with t(8;21)	Whole BM unsorted
AML t(11q23)/MLL	AML with t(11q23)/MLL	Whole BM unsorted
AML complex	AML with complex aberrant karyotype	Whole BM unsorted
HSC	Hematopoietic stem cell	Lin- CD34+ CD38- CD90+ CD45RA-
MPP	Multipotential progenitors	Lin- CD34+ CD38- CD90- 45RA-
CMP	Common myeloid progenitor cell	Lin- CD34+ CD38+ CD45RA- CD123+
GMP	Granulocyte monocyte progenitors	Lin- CD34+ CD38+ CD45RA+ CD123+
MEP	Megakaryocyte-erythroid progenitor cell	Lin- CD34+ CD38+ CD45RA- CD123-
early_PM	Early Promyelocyte	Lin- FSChi SSCint CD34- CD15int CD49dhi CD33hi CD11b- CD16-
late_PM	Late Promyelocyte	Lin- FSChi SSChi CD34- CD15hi CD49dhi CD33hi CD11b- CD16-
MY	Myelocyte	Lin- FSChi SSChi CD34- CD15hi CD49dhi CD33hi CD11bhi CD16-
MM	Metamyelocytes	Lin- FSChi SSChi CD34- CD15hi CD49d- CD33- CD11bhi CD16-
BC	Band cell	Lin- FSChi SSChi CD34- CD15hi CD49d- CD33- CD11bhi CD16int
PMN	Polymorphonuclear cells	Lin- FSChi SSChi CD34- CD15hi CD49d- CD33- CD11bhi CD16hi
Mono	Monocytes	CD14+ CD16-

b

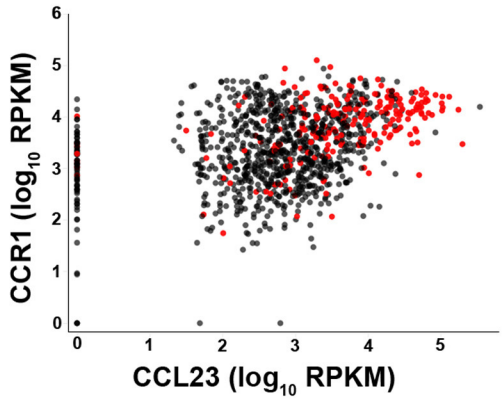

c

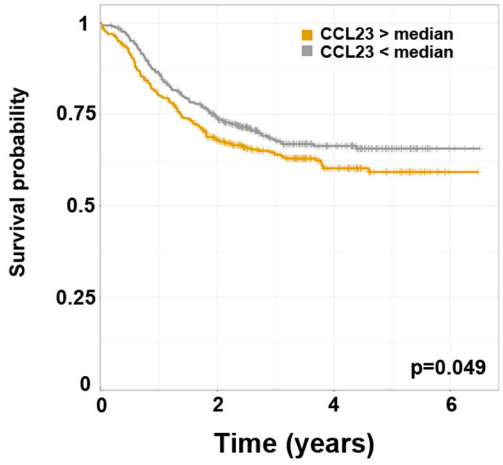

Supplemental figure 9

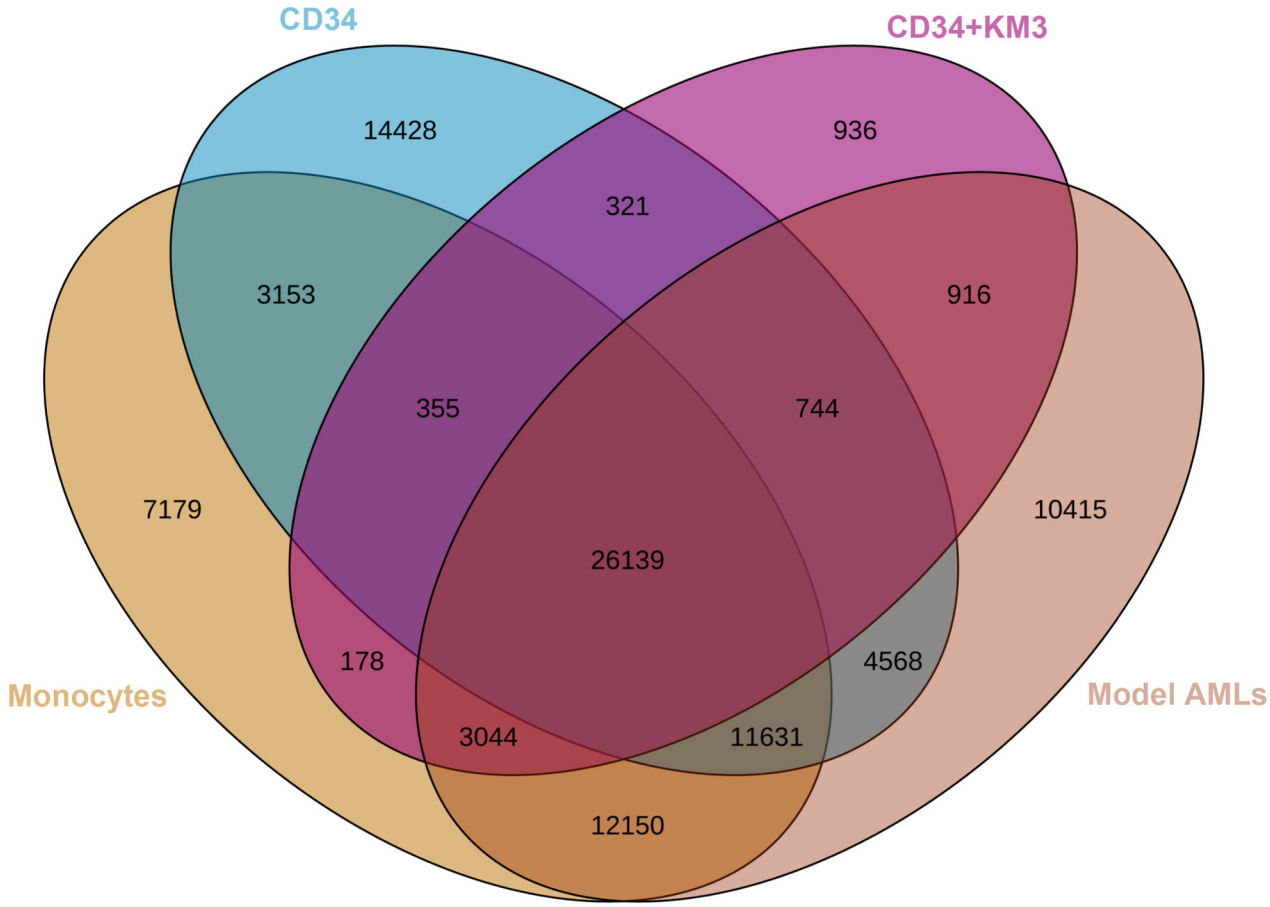

Supplemental figure 10

Rank	Motif	Name	P-value	log P-pvalue	q-value (Benjamini)	# Target Sequences with Motif	% of Targets Sequences with Motif	# Background Sequences with Motif	% of Background Sequences with Motif
1		SpiB(ETS)/OCILY3-SPIB-ChIP-Seq(GSE56857)/Homer	1e-1014	-2.336e+03	0.0000	1917.0	18.41%	965.9	2.48%
2		PU.1(ETS)/ThioMac-PU.1-ChIP-Seq(GSE21512)/Homer	1e-986	-2.272e+03	0.0000	2464.0	23.66%	1791.8	4.59%
3		ELF5(ETS)/T47D-ELF5-ChIP-Seq(GSE30407)/Homer	1e-815	-1.879e+03	0.0000	2771.0	26.61%	2751.2	7.05%
4		PU.1:IRF8(ETS:IRF)/pDC-Irf8-ChIP-Seq(GSE66899)/Homer	1e-676	-1.559e+03	0.0000	1443.0	13.86%	833.7	2.14%
5		ETS1(ETS)/Jurkat-ETS1-ChIP-Seq(GSE17954)/Homer	1e-604	-1.393e+03	0.0000	2792.0	26.81%	3510.2	9.00%
6		IRF8(IRF)/BMDM-IRF8-ChIP-Seq(GSE77884)/Homer	1e-572	-1.318e+03	0.0000	1726.0	16.57%	1473.7	3.78%
7		ELF3(ETS)/PDAC-ELF3-ChIP-Seq(GSE64557)/Homer	1e-571	-1.316e+03	0.0000	2416.0	23.20%	2812.1	7.21%
8		EHF(ETS)/LoVo-EHF-ChIP-Seq(GSE49402)/Homer	1e-549	-1.265e+03	0.0000	3317.0	31.85%	5024.3	12.88%
9		JunB(bZIP)/DendriticCells-JunB-ChIP-Seq(GSE36099)/Homer	1e-533	-1.228e+03	0.0000	1895.0	18.19%	1885.8	4.83%
10		ETV1(ETS)/GIST48-ETV1-ChIP-Seq(GSE22441)/Homer	1e-528	-1.218e+03	0.0000	3147.0	30.22%	4698.4	12.04%
11		Fra1(bZIP)/BT549-Fra1-ChIP-Seq(GSE46166)/Homer	1e-527	-1.215e+03	0.0000	1888.0	18.13%	1888.7	4.84%
12		BATF(bZIP)/Th17-BATF-ChIP-Seq(GSE39756)/Homer	1e-527	-1.214e+03	0.0000	2099.0	20.15%	2306.3	5.91%
13		Atf3(bZIP)/GBM-ATF3-ChIP-Seq(GSE33912)/Homer	1e-527	-1.214e+03	0.0000	2120.0	20.36%	2349.8	6.02%
14		AP-1(bZIP)/ThioMac-PU.1-ChIP-Seq(GSE21512)/Homer	1e-514	-1.184e+03	0.0000	2227.0	21.38%	2618.8	6.71%
15		Fra2(bZIP)/Striatum-Fra2-ChIP-Seq(GSE43429)/Homer	1e-494	-1.139e+03	0.0000	1663.0	15.97%	1564.0	4.01%
16		Etv2(ETS)/ES-ER71-ChIP-Seq(GSE59402)/Homer(0.967)	1e-463	-1.067e+03	0.0000	2448.0	23.50%	3318.9	8.51%
17		PU.1-IRF(ETS:IRF)/Bcell-PU.1-ChIP-Seq(GSE21512)/Homer	1e-453	-1.045e+03	0.0000	3438.0	33.01%	5878.9	15.07%
18		Fli1(ETS)/CD8-FLI-ChIP-Seq(GSE20898)/Homer	1e-452	-1.041e+03	0.0000	2558.0	24.56%	3628.8	9.30%
19		GABPA(ETS)/Jurkat-GABPa-ChIP-Seq(GSE17954)/Homer	1e-451	-1.039e+03	0.0000	2245.0	21.56%	2905.8	7.45%
20		ERG(ETS)/VCaP-ERG-ChIP-Seq(GSE14097)/Homer	1e-449	-1.034e+03	0.0000	3421.0	32.85%	5862.2	15.02%
21		Fosl2(bZIP)/3T3L1-Fosl2-ChIP-Seq(GSE56872)/Homer	1e-431	-9.941e+02	0.0000	1256.0	12.06%	1016.8	2.61%
22		Jun-AP1(bZIP)/K562-cJun-ChIP-Seq(GSE31477)/Homer	1e-370	-8.536e+02	0.0000	998.0	9.58%	739.7	1.90%
23		CTCF(Zf)/CD4+-CTCF-ChIP-Seq(Barski_et_al.)/Homer	1e-354	-8.173e+02	0.0000	579.0	5.56%	222.5	0.57%
24		IRF3(IRF)/BMDM-Irf3-ChIP-Seq(GSE67343)/Homer	1e-305	-7.023e+02	0.0000	1333.0	12.80%	1527.2	3.91%
25		EWS:ERG-fusion(ETS)/CADO_ES1-EWS:ERG-ChIP-Seq(SRA014231)/Homer	1e-296	-6.817e+02	0.0000	1892.0	18.17%	2813.9	7.21%

Supplemental figure 11

-

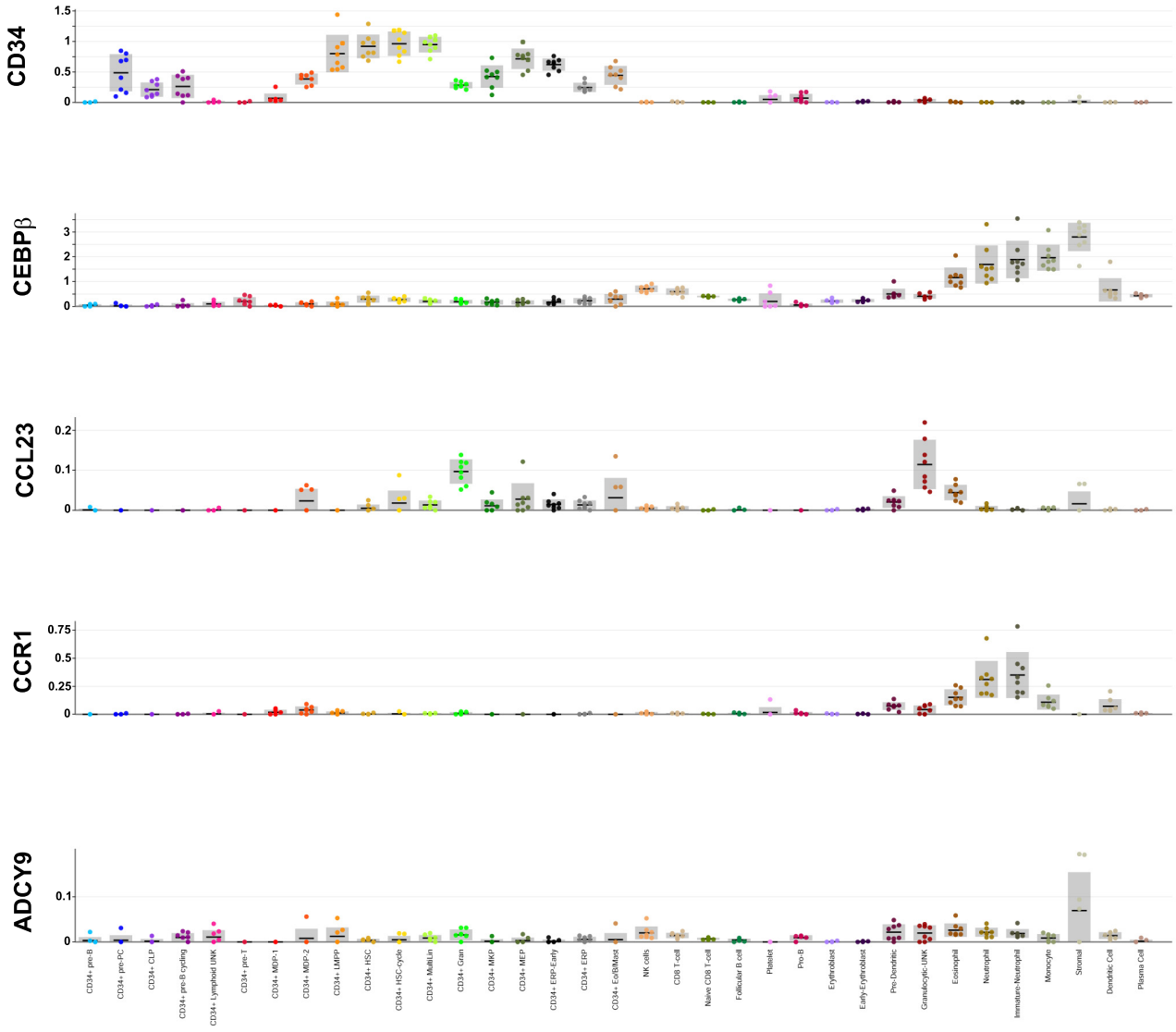

Supplemental figure 12

Supplementary Figure 1 | Gene set enrichment analysis of KMT2A-MLLT3 expressing CD34$^+$ cells. After performing differential gene expression analysis using RNA-seq data from human CD34$^+$ and CD34$^+$ cells transduced with the KMT2A-MLLT3 gene fusion a ranked list of significantly altered gene was used for gene set enrichment analysis (GSEA) to match to published signatures. **(A)** Genes whose expression was lost clearly matched HSC signatures while genes that increased in expression **(B)** matched very closely published targets of HOXA9 and MEIS1.

Supplementary Figure 2 | Expression of various transcription factor families in model leukemia stages. Box plots of gene expression data (log_2 of FPKM values) from three different stages in model leukemia system are shown for several transcription factor families. Transcription factor families include **(A)** FOS and FOSL, **(B)** MAF and JUN, **(C)** CEBP and **(D)** ETS.

Supplementary Figure 3 | Intra- and inter-individual reproducibility. Scatterplots for pair-wise comparisons of percentage levels of methylation in different samples used (CLT_1/2 = CD34$^+$ controls, CD34MA9_1/2 = CD34+KM3, PAT_1/2 = patient samples 1 and 2). Numbers on upper right corners denote pair-wise Pearson correlation scores. The histograms on the diagonal are percentage methylation histograms.

Supplementary Figure 4 | Descriptive statistics of methylation data. (A) Histogram of read coverage per cytosine for the KM3-AML model (one example of the 2 biological replicates). **(B)** Pie chart of the alignment statistics for the KM3-AML model (one of the 2 biological replicates). **(C)** Percentage of methylated (red) and unmethylated (grey) cytosines (compare to all cytosine

loci in the genome) for the control $CD34^+$, CD34+KM3 and model AML cells. **(D)** Composition of all methylated cytosine loci (mCpG:grey; mCHH: black; mCHG: dark grey) in the control $CD34^+$, CD34+KM3 and model AML cells. **(E)** Percentage of differentially methylated cytosines (DMCs) in the 22 chromosomes, in model AML (left panel) or in patient AML (right panel), compared to $CD34^+$ cells (pink : hypermethylation; green : hypomethylation)**.**

Supplementary Figure 5 | Distribution in functional genomic elements of DMCs associated to the development of KM3 translocated model patients AMLs. Differentially methylated cytosines (DMCs) from each pairwise comparison are indicated under each pie chart. Gene annotation is taken from Refseq (hg19) at UCSC genome browser. Promoter regions were defined as the 1000 bp upstream of the annotated transcription start site.

Supplementary Figure 6 | Distribution in and around CpG islands of DMCs associated to the development of KM3 translocated model patients AMLs. Differentially methylated cytosines (DMCs) from each pairwise comparison are indicated under each pie chart. CpG islands (CpGi) are defined from RefSeq (hg19) downloaded from the UCSC genome browser. The CpGi shores and CpGi shelves sequences up to 2k bp and 4k bp distant, respectively.

Supplementary Figure 7 | DNA methylation in TFBS sites. (A) To identify consistently differentially methylated cytosines (DMCs), positions were first limited to those in the genome that had sufficient coverage to assess changes (>8 reads). These positions were then filtered for those where there was >40% loss of methylation in both CD34+KM3 and model AMLs (12,710

final positions). These DMCs positions were then compared to the conserved transcription factor binding site track ("TFBS conserved") in the UCSC human genome browser to identify transcription factors (TFs) whose accessibility might be impacted by methylation changes. **(B)** The interactive GOnet website was then used to take the TFs from **(A)** and build a network based on shared hierarchical GO terms (q-value threshold <=0.0001). The gene nodes in the network were then automatically coloured by their expression in normal bone marrow using data from the Human Protein Atlas. The bottom right portion of the graph shows an enrichment in GO-terms associated with hematopoietic/stem cell fate, and myeloid differentiation involving TFs that are all highly expressed in bone marrow.

Supplementary Figure 8 | Genome-wide distribution of histone modifications in model leukemias. (A) The spatial distribution of H3K4me3 and H3K79me2 was plotted across average genes in each of the three model leukemia stages, as well as by ranked enrichment in individual genes, using EaSeq package. **(B)** Histone modifications across average genes are shown with genes binned into high, medium and low gene expression levels.

Supplementary Figure 9 | Expression of the CCL23 gene in leukemic and normal blood cells.

(**A**) Normalized gene expression data for CCL23 from previously published studies of normal and leukemic samples is shown. The table in the lower panel details the sample abbreviations and the immunophenotype for each of the samples represented. (**B**) Expression of CCR1 and CCL23 in the TARGET pediatric AML cohort, with KMT2A translocated patients coloured in red. (**C**)

Kaplan-Meier survival curve based on expression of CCL23 above/below the median from the TARGET AML cohort.

Supplementary Figure 10 | Overlapping peaks in ATAC-seq data from normal and leukemic cells. Venn diagram shows the number of peaks detected by MACS2 in normal blood cells (monocytes, $CD34^+$ cells) or model leukemia stages (CD34+KM3, mAML).

Supplementary Figure 11 | Predicted transcription factor binding sites in ATAC-seq peaks. The table presents the predictive output of Homer for the top 25 transcription factors whose binding motifs are over-represented in the ATAC-seq peaks that are uniquely found in the model leukemia samples.

Supplementary Figure 12 | Single-cell expression in normal blood cells. Published single cell RNA-seq data from 35 different cell types shows the expression of 4 genes highlighted in this paper (*CEBPβ, CCR1, CCL23, ADCY9*) as well as CD34 as a cell-type specific expression control. Graphs of expression were generated by the Human Cell Atlas interactive web portal[61] and are automatically scaled to the range of expression values for each gene.

Supplemental Table 1 - Summary of pediatric patients in this study

ID	Age	FAB	Blast % (BM)	Karyotype
Ped_159	1 yr	M5A	70	46,XX,der(9)t(9;11)(p22;q23)del(9)(p21)[20]
Ped_111	5 yr	M5A	85	48,XX,+8,+8,t(9;11)(p22;q23)[20]
Ped_144	13 yr	M5A	90	46,XX,t(9;11)(p22;q23)[5]/47,XX,+8,t(9;11)(p22;q23)[16]

Supplementary table 2 - Gene expression changes in chromatin modifying enzymes

Gene	CD34	CD34+MA9	model AML	patient AML	mononuclear
KDM1A	46.471	18.755	22.589	24.626	15.197
KDM1B	12.039	16.921	11.720	17.662	10.199
KDM2A	37.539	20.886	36.493	37.906	42.284
KDM2B	16.744	13.540	21.444	17.248	10.929
KDM3A	17.257	28.231	14.068	22.170	23.684
KDM3B	20.863	23.689	19.920	17.813	17.052
KDM4A	14.711	17.619	18.516	19.248	5.202
KDM4B	11.361	22.256	8.988	9.353	13.776
KDM4C	6.737	8.488	6.843	7.315	11.092
KDM4D	0.286	0.138	0.041	0.076	0.062
KDM4DL	0.160	0.000	0.016	0.026	0.018
KDM5A	9.035	10.903	8.611	10.799	8.188
KDM5B	33.772	10.942	6.980	12.961	9.377
KDM5C	24.483	19.851	19.540	24.656	18.954
KDM5D	17.998	35.667	11.306	0.003	9.699
KDM6A	8.392	7.614	8.840	13.332	11.476
KDM6B	18.730	16.113	32.582	18.426	30.926
DNMT1	35.691	20.617	50.089	29.453	18.929
DNMT3A	20.330	8.424	6.115	6.457	10.768
DNMT3B	17.454	1.187	1.685	1.100	1.082
DNMT3L	0.225	0.046	0.029	0.094	0.138
TET1	0.723	0.173	0.369	0.406	0.378
TET2	4.916	8.426	12.149	10.080	5.934
TET3	9.040	15.189	12.756	9.543	13.917
HDAC1	77.530	45.049	52.593	57.414	45.955
HDAC10	21.643	18.454	25.500	30.143	19.384
HDAC11	2.707	0.846	0.987	1.490	0.992
HDAC2	17.853	10.142	12.326	13.356	6.523
HDAC3	34.843	28.302	42.277	36.867	23.097
HDAC4	2.440	7.822	12.053	12.984	3.985
HDAC5	18.406	10.859	18.155	17.600	16.219
HDAC6	28.259	14.481	22.566	24.029	16.753
HDAC7	57.189	11.657	18.272	18.399	44.518
HDAC8	5.560	4.548	4.139	3.364	1.891
HDAC9	2.568	0.928	4.653	6.201	2.599
SUV39H1	6.791	4.060	9.971	5.327	3.284
SUV39H2	3.267	1.604	1.370	2.067	1.090
JMJD1C	17.121	8.540	61.059	58.157	22.144
JMJD4	6.837	4.110	3.535	4.776	1.887
JMJD5	2.456	1.309	1.729	1.594	1.630
JMJD6	8.376	7.191	18.882	15.544	12.219
JMJD7	8.551	7.777	10.008	7.202	13.590
JMJD8	21.773	12.187	22.350	25.104	13.826

Supplemental Table 3 - Genes with correlated gene expression and active histone modifications.

Chromosome	Start	End	Strand	Gene
chr8	9757574	9760839	+	LOC157627
chr2	219646472	219680016	+	CYP27A1
chr17	56270089	56282535	+	EPX
chr19	7733972	7735340	+	RETN
chr1	153362508	153363664	+	S100A8
chr19	7741943	7744719	+	C19orf59
chr1	182761394	182798588	+	NPL
chr3	46243200	46249832	+	CCR1
chr5	140011313	140013286	+	CD14
chr11	124933013	124960412	+	SLC37A2
chr19	55385549	55401839	+	FCAR
chr17	78194200	78227308	+	SLC26A11
chr9	120466460	120479766	+	TLR4
chr1	153330330	153333503	+	S100A9
chr2	218990013	219001976	+	CXCR2
chr13	111175413	111214071	+	RAB20
chr5	179220986	179223513	+	LTC4S
chr16	31271288	31344213	+	ITGAM
chr6	151815175	151942328	+	C6orf97
chr19	4537227	4540036	+	LRG1
chr2	138721808	138773934	+	HNMT
chr13	31309669	31338556	+	ALOX5AP
chr19	18284579	18288927	+	IFI30
chr19	51645558	51656783	+	SIGLEC7
chr19	52145806	52150132	+	SIGLEC14
chr5	122181160	122344902	+	SNX24
chr21	34442450	34444728	+	OLIG1
chr19	51628137	51639520	+	SIGLEC9
chr5	135364584	135399507	+	TGFBI
chr18	61582745	61602476	+	SERPINB10
chr14	88471468	88481155	+	GPR65
chr6	160390131	160527583	+	IGF2R
chr14	55595935	55612148	+	LGALS3
chr12	6898638	6929976	+	CD4
chr1	158801168	158819270	+	MNDA
chr3	122044011	122060815	+	CSTA
chr17	42422491	42430470	+	GRN
chr7	150497854	150502208	+	TMEM176A
chr16	31366509	31394318	+	ITGAX
chr17	80186293	80197369	+	SLC16A3
chr19	55174124	55179846	+	LILRB4
chr8	74903564	74941307	+	LY96
chr12	69742134	69748013	+	LYZ

Chromosome	Start	End	Strand	Gene
chr11	59824101	59838588	+	MS4A3
chr5	149432854	149492935	+	CSF1R
chr12	100967489	101018685	+	GAS2L3
chr9	80912059	80945009	+	PSAT1
chr3	169755735	169803183	+	GPR160
chr3	132036211	132087146	+	ACPP
chr19	36395303	36399211	+	TYROBP
chr1	161185087	161189038	+	FCER1G
chr14	65171193	65211060	+	PLEKHG3
chr5	150827163	150871940	+	SLC36A1
chr22	17597189	17602257	+	CECR6
chr11	72929344	72947395	+	P2RY2
chr14	25042724	25045466	+	CTSG
chr3	46395235	46402413	+	CCR2
chr17	78183079	78194199	+	SGSH
chr7	27220776	27224835	+	HOXA11
chrX	12924739	12941288	+	TLR8
chr19	852291	856246	+	ELANE
chr8	48649476	48650726	+	CEBPD
chr14	21249210	21250626	+	RNASE6
chr16	28505993	28510282	+	APOB48R
chr3	69788586	70017488	+	MITF
chr11	58976061	58980494	+	MPEG1
chr12	129338081	129469509	+	GLT1D1
chr16	50731050	50766987	+	NOD2
chr11	48002110	48192394	+	PTPRJ
chr5	82767493	82878122	+	VCAN
chr18	9708228	9862553	+	RAB31
chr16	85061410	85127828	+	KIAA0513
chr20	1874813	1920540	+	SIRPA
chr12	32655041	32798984	+	FGD4
chr19	827831	832017	+	AZU1
chr1	12227060	12269277	+	TNFRSF1B
chr17	55055468	55084129	+	SCPEP1
chr1	28473677	28520437	+	PTAFR
chr20	48807376	48809212	+	CEBPB
chr10	45455219	45490172	+	RASSF4
chr14	76044940	76114512	+	FLVCR2
chr5	53813589	53842416	+	SNX18
chr7	27225027	27228912	+	HOXA11-AS1
chr17	64298926	64806862	+	PRKCA
chr16	1988234	1993294	+	SEPX1
chr10	65281123	65384883	+	REEP3
chr4	15704573	15733796	+	BST1
chr22	17565851	17596584	+	IL17RA

Chromosome	Start	End	Strand	Gene
chr20	23614294	23618574	+	CST3
chr3	42695176	42709072	+	ZBTB47
chr19	50015536	50029685	+	FCGRT
chr5	73980969	74017030	+	HEXB
chr10	60094739	60130509	+	UBE2D1
chr7	76822688	76829150	+	FGL2
chr17	28705942	28796675	+	CPD
chr11	65543378	65547822	+	DKFZp761E198
chr7	48128355	48148330	+	UPP1
chr1	40361096	40367687	+	MYCL1
chr17	15848231	15879210	+	ADORA2B
chr11	60145958	60163426	+	MS4A7
chr19	13947401	13947473	+	MIR23A
chr5	66478104	66492617	+	CD180
chr11	61447905	61514474	+	DAGLA
chr21	34638672	34669520	+	IL10RB
chr2	219246752	219261617	+	SLC11A1
chr6	35310335	35395968	+	PPARD
chr1	109822176	109825790	+	PSRC1
chr17	47287589	47300587	+	ABI3
chr20	30639991	30689657	+	HCK
chr12	113659260	113736389	+	TPCN1
chr12	40618813	40763086	+	LRRK2
chr8	20054704	20079207	+	ATP6V1B2
chr5	49961733	50142356	+	PARP8
chr15	66994674	67074337	+	SMAD6
chr5	14581891	14616287	+	FAM105A
chr3	53195223	53226733	+	PRKCD
chr17	4901243	4931694	+	KIF1C
chr17	72690452	72709108	+	CD300LF
chr17	42634812	42638630	+	FZD2
chr11	10326642	10328923	+	ADM
chr19	16771938	16799816	+	TMEM38A
chr6	151773422	151791232	+	C6orf211
chr11	62104774	62160887	+	ASRGL1
chr10	65224989	65226322	+	LOC84989
chr1	150521898	150533412	+	ADAMTSL4
chr9	108006929	108153682	+	SLC44A1
chr3	71820806	71834357	+	PROK2
chr8	21766384	21771205	+	DOK2
chr11	117857106	117872199	+	IL10RA
chr13	49063099	49107316	+	RCBTB2
chr5	79783800	79838206	+	FAM151B
chr1	28199055	28213193	+	C1orf38
chr12	109015680	109027670	+	SELPLG

Chromosome	Start	End	Strand	Gene
chr16	84599204	84651669	+	COTL1
chr19	36393382	36395173	+	HCST
chr9	36136742	36163903	+	GLIPR2
chr21	45138978	45182188	+	PDXK
chr1	178063129	178448648	+	RASAL2
chr4	154605441	154627242	+	TLR2
chr5	148206156	148208197	+	ADRB2
chr1	154975112	154990999	+	ZBTB7B
chr4	7045156	7059677	+	TADA2B
chr6	3020390	3025005	+	LOC401233
chr1	153507076	153508717	+	S100A6
chr9	128509617	128729655	+	PBX3
chr12	10124008	10138194	+	CLEC12A
chr19	38810484	38819649	+	KCNK6
chr3	39304985	39323226	+	CX3CR1
chr12	56078395	56106089	+	ITGA7
chr1	11796142	11810828	+	AGTRAP
chr1	51434367	51440306	+	CDKN2C
chr11	76571917	76734850	+	ACER3
chr19	33685599	33699569	+	LRP3
chr11	94300474	94354587	+	PIWIL4
chr6	11538511	11583757	+	TMEM170B
chr22	38071613	38075809	+	LGALS1
chr17	41166622	41174459	+	VAT1
chr17	7461609	7463210	+	TNFSF13
chr5	173315331	173387313	+	CPEB4
chr3	171757418	172118492	+	FNDC3B
chr12	113860216	113876081	+	SDSL
chr10	82214038	82282391	+	TSPAN14
chr18	2847028	2914090	+	EMILIN2
chr18	46446223	46477081	+	SMAD7
chr2	111878491	111926022	+	BCL2L11
chr21	45773484	45862964	+	TRPM2
chr2	120124504	120130122	+	DBI
chr1	10459085	10480201	+	PGD
chr12	132312941	132336316	+	MMP17
chr14	75745481	75748937	+	FOS
chr1	154377669	154440188	+	IL6R
chr22	35695268	35743987	+	TOM1
chr6	6588934	6655216	+	LY86
chr11	67806462	67818366	+	TCIRG1
chr5	142150292	142608572	+	ARHGAP26
chr20	62526455	62567384	+	DNAJC5
chr15	77287465	77329671	+	PSTPIP1
chr10	64893007	64914786	+	NRBF2

Chromosome	Start	End	Strand	Gene
chr11	2466221	2870340	+	KCNQ1
chr15	63413999	63434260	+	LACTB
chr17	33570086	33594761	+	SLFN5
chr1	151584662	151671559	+	SNX27
chr1	53392901	53517289	+	SCP2
chr15	92396938	92715665	+	SLCO3A1
chr11	94277017	94283064	+	FUT4
chr19	33182867	33204702	+	NUDT19
chr18	47013413	47013644	+	C18orf32
chr21	37536839	37666572	+	DOPEY2
chr1	92940318	92952433	+	GFI1
chr9	115513134	115637267	+	SNX30
chr1	179851420	179889211	+	TOR1AIP1
chr10	75672043	75677258	+	PLAU
chr13	113344643	113541482	+	ATP11A
chr11	32851489	32876105	+	PRRG4
chr13	32605437	32870776	+	FRY
chr10	101419263	101468504	+	ENTPD7
chr20	58630980	58648008	+	C20orf197
chr2	160654643	160654766	+	CD302
chr11	14665269	14893604	+	PDE3B
chr9	94171327	94186144	+	NFIL3
chr1	151129105	151132223	+	TNFAIP8L2
chr16	28996147	29002104	+	LAT
chr19	840985	848175	+	PRTN3
chr12	125478194	125510349	+	BRI3BP
chr19	51728335	51743274	+	CD33
chr3	58318617	58410878	+	PXK
chr17	57697050	57774317	+	CLTC
chr1	201951766	201975275	+	RNPEP
chr22	38035684	38052050	+	SH3BP1
chr5	175085040	175113245	+	HRH2
chr18	61637263	61656608	+	SERPINB8
chr6	150070831	150132557	+	PCMT1
chr19	51874874	51875960	+	NKG7
chr2	48541795	48606434	+	FOXN2
chr19	33790840	33793430	+	CEBPA
chr9	140172280	140177093	+	C9orf167
chr1	36273828	36321188	+	EIF2C4
chr1	40420784	40435628	+	MFSD2A
chr8	8860314	8890849	+	ERI1
chr6	127588020	127609504	+	RNF146
chr5	56110900	56191978	+	MAP3K1
chr9	110247133	110252047	+	KLF4
chr19	10381517	10397291	+	ICAM1

Chromosome	Start	End	Strand	Gene
chr6	36973423	36996845	+	FGD2
chr12	4430359	4469190	+	C12orf5
chr11	64107690	64125006	+	CCDC88B
chr17	7076751	7082883	+	ASGR1
chr4	2794750	2842823	+	SH3BP2
chr9	139971953	139978990	+	UAP1L1
chr11	6232564	6255941	+	FAM160A2
chr14	103592664	103603776	+	TNFAIP2
chr16	30483983	30534506	+	ITGAL
chr16	2479395	2508859	+	CCNF
chr12	45609790	45834187	+	ANO6
chr6	31626075	31628549	+	C6orf47
chr7	38299244	38313248	+	TARP
chr7	143078360	143088204	+	ZYX
chr1	150524405	150524490	+	MIR4257
chr17	46184920	46200105	+	SNX11
chr4	148653453	148993927	+	ARHGAP10
chr9	132575221	132586441	+	TOR1A
chr3	196466728	196559518	+	PAK2
chr16	30960405	30966259	+	ORAI3
chr9	82186878	82341656	+	TLE4
chr3	190231840	190374986	+	IL1RAP
chr1	2160134	2241652	+	SKI
chr10	17270258	17279592	+	VIM
chr1	247579458	247612406	+	NLRP3
chr12	21590538	21624182	+	PYROXD1
chr11	73087405	73108519	+	RELT
chr16	68119269	68262449	+	NFATC3
chr19	6531010	6535939	+	TNFSF9
chr2	131113580	131132982	+	PTPN18
chr17	57918627	57918698	+	MIR21
chr1	111729801	111743281	+	DENND2D
chr4	177241090	177253396	+	SPCS3
chr4	106067943	106200958	+	TET2
chr12	121124949	121139667	+	MLEC
chr7	30323923	30407308	+	ZNRF2
chr3	52740049	52742197	+	SPCS1
chr1	15736391	15756839	+	EFHD2
chr9	100174302	100258405	+	TDRD7
chr9	140500096	140509783	+	ARRDC1
chr16	23847300	24231932	+	PRKCB
chr10	102790996	102800998	+	SFXN3
chr2	74425690	74442424	+	MTHFD2
chr5	148724977	148734146	+	GRPEL2
chr14	74960450	74962271	+	ISCA2

Chromosome	Start	End	Strand	Gene
chr19	16244838	16269377	+	HSH2D
chr16	21610856	21668792	+	METTL9
chr1	153516095	153518282	+	S100A4
chr15	45927256	45983479	+	SQRDL
chr22	50968838	50971008	+	ODF3B
chr19	12902310	12904125	+	JUNB
chr19	571325	583493	+	BSG
chr10	129705325	129884164	+	PTPRE
chr11	33279168	33375939	+	HIPK3
chr6	31465855	31478901	+	MICB
chr9	128024111	128127290	+	GAPVD1
chr11	63742079	63744015	+	COX8A
chrX	100663121	100663295	+	HNRNPH2
chr17	1619817	1641893	+	WDR81
chr16	50099881	50139375	+	HEATR3
chr17	21030258	21094836	+	DHRS7B
chr17	2496923	2588909	+	PAFAH1B1
chr22	44568836	44603035	+	PARVG
chr13	25875666	25916561	+	NUPL1
chr15	76135622	76193388	+	UBE2Q2
chr11	65343509	65360116	+	EHBP1L1
chr9	130823512	130829599	+	NAIF1
chr5	133984479	134063601	+	SEC24A
chr15	57592563	57599967	+	LOC283663
chr15	31619083	31670102	+	KLF13
chr9	139924626	139926449	+	FUT7
chr10	75757872	75879914	+	VCL
chr14	20937538	20946165	+	PNP
chr16	2261603	2264822	+	PGP
chr7	2273926	2281833	+	FTSJ2
chr2	234263153	234380743	+	DGKD
chr2	218923878	218926013	+	CXCR2P1
chr14	97263684	97347951	+	VRK1
chr16	11348274	11350039	+	SOCS1
chr12	66696356	66731958	+	HELB
chr15	32812049	32825942	+	LOC100288615
chr18	9913955	9960018	+	VAPA
chr2	28113557	28561767	+	BRE
chr12	54756229	54758270	+	GPR84
chr4	174292093	174298683	+	SAP30
chr16	31085743	31094744	+	ZNF646
chr19	33793763	33795963	+	LOC80054
chr5	134784558	134788089	+	TIFAB
chr20	30193092	30194313	+	ID1
chr17	34900737	34946276	+	GGNBP2

Chromosome	Start	End	Strand	Gene
chr4	2932288	2936586	+	MFSD10
chr13	73302042	73329539	+	C13orf34
chr16	4853204	4897303	+	GLYR1
chr1	179051112	179065129	+	TOR3A
chr1	38326369	38412729	+	INPP5B
chr16	3072626	3074287	+	HCFC1R1
chr1	28218049	28241236	+	RPA2
chr5	131630145	131679899	+	SLC22A4
chr7	156931655	157062066	+	UBE3C
chr6	26538572	26547164	+	HMGN4
chr15	85291818	85349663	+	ZNF592
chr5	141018869	141030986	+	FCHSD1
chr11	64073044	64084164	+	ESRRA
chr12	12870302	12875305	+	CDKN1B
chr22	21996542	21998588	+	SDF2L1
chr16	85932774	85956211	+	IRF8
chr12	46123620	46301819	+	ARID2
chr1	109756515	109780804	+	SARS